



This page is left blank

This page is left blank

## ULTRASONIC WELD TESTING AND IMAGING USING PORTABLE AUTOMATED ARM

A. CHAHBAZ, A. CYR, R. SICARD  
A. PELLETIER AND M. BRASSARD

TEKTREND INTL , NDT TECHNOLOGY AND DEVELOPMENT  
2001 ST REGIS BLVD , MONTREAL, QUE , H9B 2M9  
research@tektrend.com

DR. J. R. MATTHEWS

DOCKYARD LABORATORY ATLANTIC  
DREA, HALIFAX, N S B3K 5X5  
jim.matthews@drea.dnd.ca

### ABSTRACT

Automated and manual ultrasonic techniques are rapidly becoming as popular as conventional radiographic techniques for weld testing applications. However, for automated ultrasonic techniques, inspection cycle time and defect/data interpretation represent important factors.

In this work, we describe the use of portable automated PC-based ultrasonic scanner to inspect simulated and real naval construction welds. The system is a self-contained single unit in which all electronic boards are mounted in the system server workstation. The system offers advanced analysis and interpretation capabilities, and can display the raw and interpreted inspection results in a realistic 3D representation.

We also examine the resulting scan images from two inspection setups used to improve inspection reliability and defect interpretation in terms of detectability of weld defects. We then averaged and reconstructed the images using a Syntactic Aperture Focusing Technique SAFT technique with an attenuation correction factor introduced to improve resolution for long propagation paths.

The Syntactic Aperture Focusing Technique (SAFT) makes it possible to increase the signal-to-noise ratio by averaging several shifted reflections from the same defect point. Lateral resolution is therefore improved, especially for long probe-to-defect distances. Moreover, the resolution remains constant along the beam axis, avoiding beam width perturbations and providing the user with a reconstructed image that makes defect interpretation easier.

## INTRODUCTION

The three most popular methods for weld inspection are Radiography, Ultrasonic Angle Beam Pulse-Echo and Time-of-Flight Diffraction. The last two methods have their own advantages and drawbacks, and do not provide full characterization of weld defects. Advanced processing techniques such as SAFT, are required to assist in characterization and precise flaw imaging.

In this work, we investigate multi-path SAFT algorithm using Ultrasonic Angle Beam Pulse-Echo to detect common pipeline weld defects (lack of fusion, lack of penetration and slag inclusion) and compare it to TOFD and time-of-flight results. Using beam width limitation with the implemented SAFT algorithm, we achieved reasonable computation time for SAFT imaging. And to improve the ultrasonic beam resolution, an attenuation correction factor was introduced.

## NDI TECHNIQUES FOR WELD EVALUATION

Manual and automated ultrasonic techniques are rapidly becoming as popular as conventional radiographic techniques. They offer great potential for weld inspection since they can be employed on in service complex welded components. The most commonly used techniques are Ultrasonic Angle Beam Pulse-Echo and Time-of-Flight Diffraction. The advantages and drawbacks of these techniques are described in Table 1:

*Table 1. Advantages and drawbacks of ultrasonic PE and TOFD*

<b>Pulse-Echo</b>
<u>Advantages</u>
<ul style="list-style-type: none"> <li>▪ Good sizing accuracy in the weld axis.</li> <li>▪ Excellent POD for various well oriented defects.</li> </ul>
<u>Drawbacks</u>
<ul style="list-style-type: none"> <li>▪ Very sensitive to defect orientation.</li> <li>▪ Weak response with off-angle planar and volumetric flaws.</li> <li>▪ Need to have “echo dynamics” information (need to use several angles simultaneously to insure defect coverage).</li> <li>▪ In some cases, poor defect-sizing information is obtained because it is based on reflected signal amplitude.</li> </ul>
<b>TOFD</b>
<u>Advantages</u>
<ul style="list-style-type: none"> <li>▪ Once a defect is identified, vertical sizing is very accurate.</li> <li>▪ Often used as a safety net for some critical defects.</li> <li>▪ Improve assessment of mismatch (high-low).</li> </ul>
<u>Drawbacks</u>
<ul style="list-style-type: none"> <li>▪ Very weak response (low SNR) from defect tips diffraction.</li> <li>▪ Classical TOFD use the assumption that the flaw is positioned symmetrically between the probes, which is rarely true.</li> <li>▪ Bad spatial resolution because of wide beam spread</li> <li>▪ Dead zone effect near the entry surface.</li> </ul>

<b>TOFD</b>	
<ul style="list-style-type: none"> <li>▪ Diffraction is more complex than reflection. Unlike PE method, it becomes difficult to analyze results for complex situations (due to mode conversions etc...).</li> <li>▪ Requires a second axis of motion (D-Scan) to define the side of weld on which the defects occurs.</li> <li>▪ Optimum probe center spacing can result in probe interference with weld cap.</li> <li>▪ Mismatch conditions can mask defects in back wall signal.</li> <li>▪ TOFD data are relatively big as multi-channel PE data.</li> </ul>	

### SAFT DATA ACQUISITION, PRINCIPLES AND ADVANTAGES

For automated ultrasonic techniques, inspection cycle time and defect/data interpretation represent important factors. The system used in our experimentation is an automated self-contained ultrasonic unit<sup>1</sup>. It features a data acquisition module, advanced analysis and interpretation capabilities, and can display the raw and interpreted inspection results in a realistic representation.

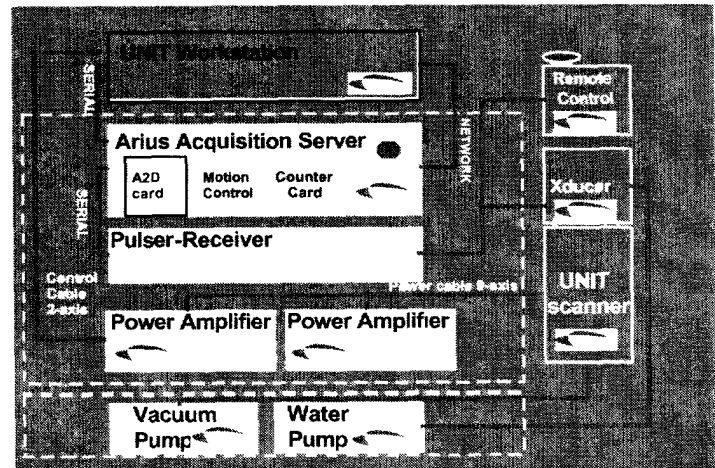
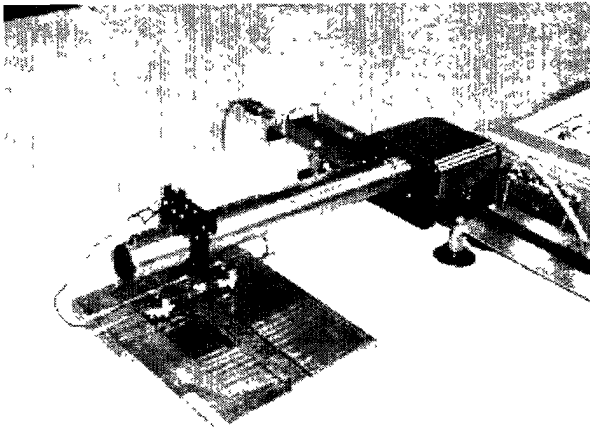


*Figure 1. System configuration and setup for weld testing*

The complete system comprises the hardware and software modules with

The software also includes simple and multi-SAFT imaging modules. The principle of conventional SAFT is to extrapolate for each transducer position and provide the sum of energy reflected and transmitted at all transducer positions (Figure 2). The extrapolation process, called back-propagation, sums up in phase signals received due to scattering on defects and signals received due stochastic noise are averaged. The great advantage of SAFT is the increase of lateral resolution, which becomes theoretically constant along the material depth. Resolution evaluation is usually provided by the estimation of the PSF (Point Spread Function) width and height resulting from SAFT processing on a point-like defect response<sup>2</sup>.

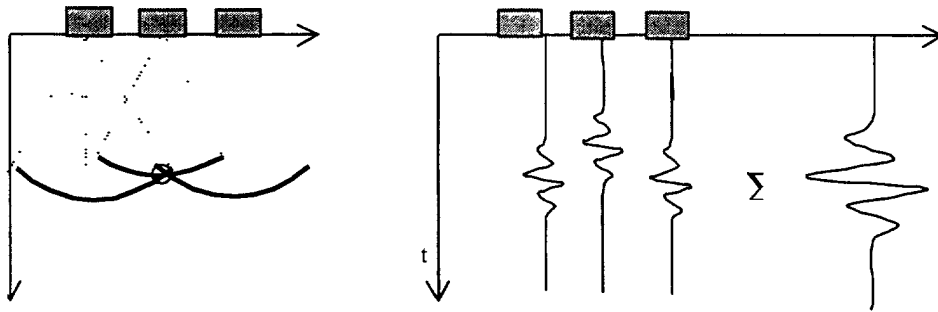
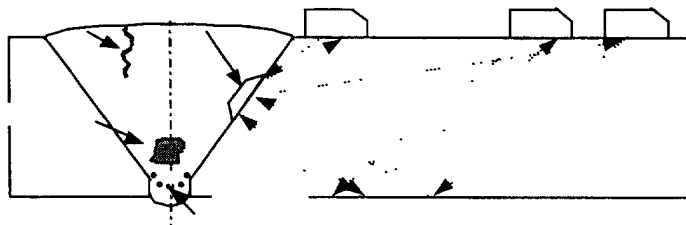


Figure 2. SAFT extrapolation principle

With SAFT imaging, resolution and signal-to-noise enhancement depend strictly on the acquisition aperture size. Therefore, *increasing the effective aperture* is the key to benefiting from SAFT's advantages. There are several practical ways to do this, including wide beam transducers, multiple wave paths including boundary reflections, pitch-catch configuration and fusion of reconstructed images acquired through different apertures. In this experimental work and since welded structures are inspected, multi-path SAFT algorithm was implemented and tested<sup>3</sup>. With this technique, multiple wave paths with boundary reflections are used to improve resolution of classical SAFT by increasing the effective aperture and information focusing. The same formulation as conventional SAFT is used for multi-path process but summated on several paths (Figure 3).



Using boundary reflections with multi-paths SAFT, long aperture paths are involved. Hence, an attenuation correction factor composed of the incident and scattering coefficients was introduced to the formulated multi-path SAFT algorithm to compensate for attenuation caused by spreading and absorption losses. Moreover, a beam width limitation was also implemented to reduce calculation time.

### INSPECTION RESULTS AND WELD EVALUATION

In the scope of this work, experiments were conducted on simulated carbon steel construction weld containing four common pipeline weld flaws (Figure 4). Tests were first performed with TOFD technique and then conventional pulse-echo method to apply the multi-path SAFT. Figure 5 shows the TOFD results presented in B-scan, using color scale level. Inspection was performed on the specimen along the Y-direction using single pass in pitch-catch at 5 MHz with 0.25" angle beam transducer to generate 65° shear waves.

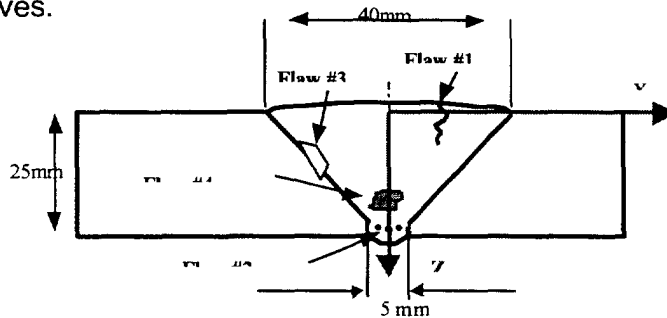


Figure 4. Weld specimen with four manufactured flaws

Table 2. Flaws dimension and location

Flaw #	Description	Distance from reference to indication			Flaw depth	Flaw height	Flaw length
		"X"	"Y"	"Z"			
1	Longitudinal crack	-0.2"	2.0"	Surface breaking	0.4"	0.5"	
2	Lack of penetration	0.0"	4.75"	0.9"	0.1"	0.4"	
3	Lack of fusion	0.35"	6.75"	0.3"	0.2"	0.5"	
4	Slag inclusion	0.0"	9.5"	0.75"	0.1"	0.5"	

Note: Flaw no. 2 is surface breaking on backwall

Results in figure 5 show the TOFD indications from the detected defects. The relatively high amplitude of the diffracted and reflected mode represents indication of flaws. Table 3 compares the measured and the real dimension of the detected flaws. Size and depth of the detected flaws with TOFD was calculated with simple Pythagorean principles<sup>4</sup>.

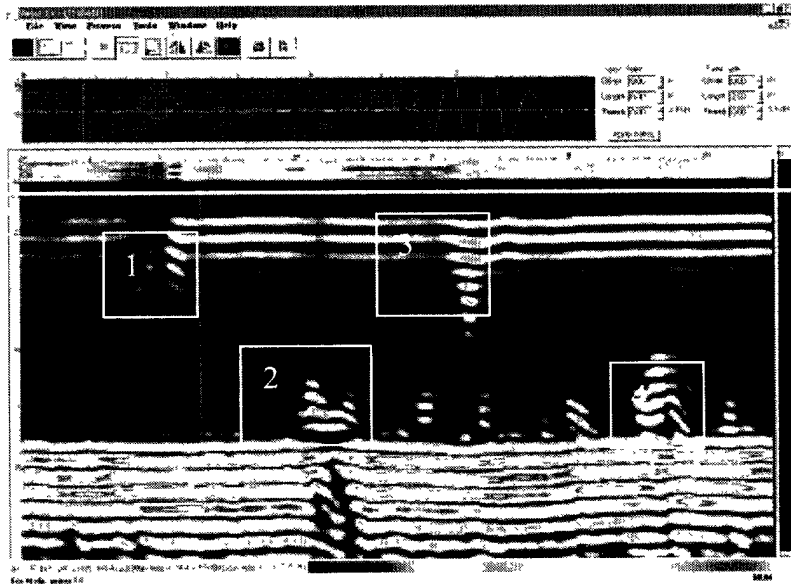


Figure 5. TOFD B-scan with color scale levels

Table 3. Flaw characterization with TOFD

Flaw	T <sub>1</sub>	T <sub>2</sub>	Depth			Height		
			Measured	Real	Error	Measured	Real	Error
1	N/a	17.14 μs	N/a	N/a	N/a	0.41"	0.4"	+0.01"
2	18.06 μs	18.48 μs	0.77"	0.9"	-0.13"	0.13"	0.1"	+0.03"
3	16.86 μs	17.54 μs	0.17"	0.3"	-0.13"	0.42"	0.2"	+0.22"
4	17.86 μs	18.48 μs	0.71"	0.75"	-0.04"	0.19"	0.1"	+0.09"

A second set of tests was performed in pulse-echo at 5 MHz with 0.25" angle beam transducer at 60°. Several lines of scans were performed and recorded. Figure 6 shows the C-scan results of the inspection displayed as conventional 0° pulse-echo scan. Each point on the C-scan originates from a different transducer position.



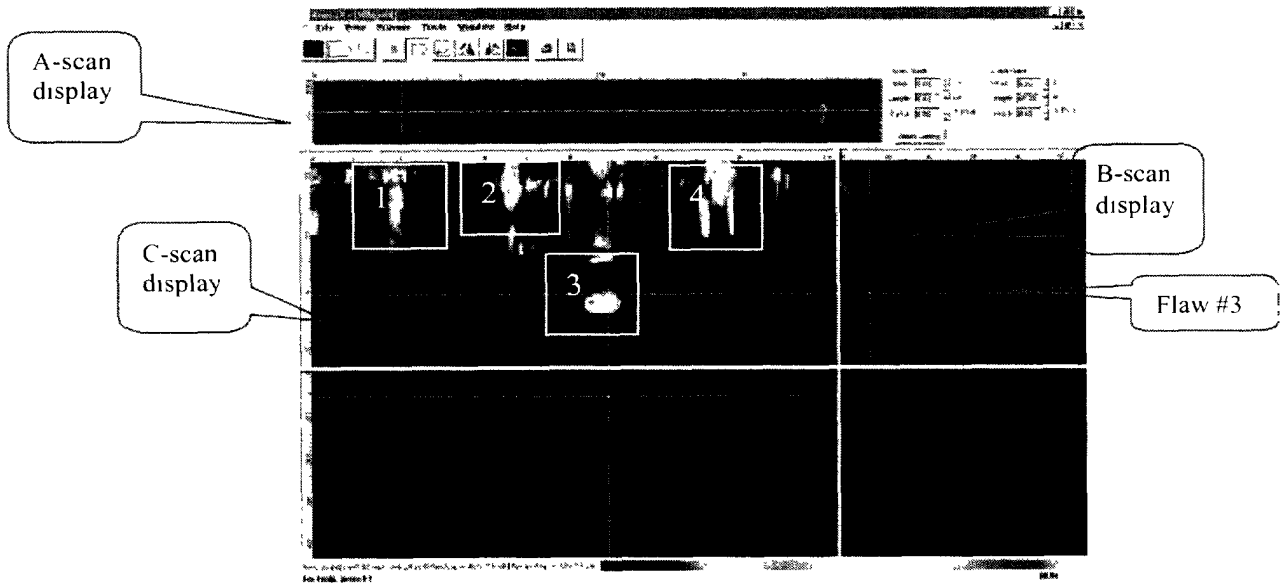


Figure 7. Pulse-echo C-Scan with color scale levels

Table 4. Flaw characterization with PE

Flaw	Depth			Height		
	Measured	Real	Error	Measured	Real	Error
1	N/a	N/a	N/a	0.35"	0.4"	0.05"
2	0.80"	0.9"	0.1"	0.11"	0.1"	0.01"
3	0.10"	0.3"	0.20"	0.13"	0.2"	0.07"
4	0.74"	0.75"	0.01"	0.26"	0.1"	0.16"

For each detected flaw with the pulse-echo setup, the time-of-flight was taken to calculate the distance and depth by simple trigonometric approach. Next, the welded construction was scanned using a 2.25 MHz 0.25" diameter probe at 45° for the Multi-path SAFT evaluation. Only flaws number 2, 3 and 4 were inspected for the multi-path SAFT. Flaw 1 is not deep enough; thus, with the SAFT we could obtain any increase in the lateral resolution.

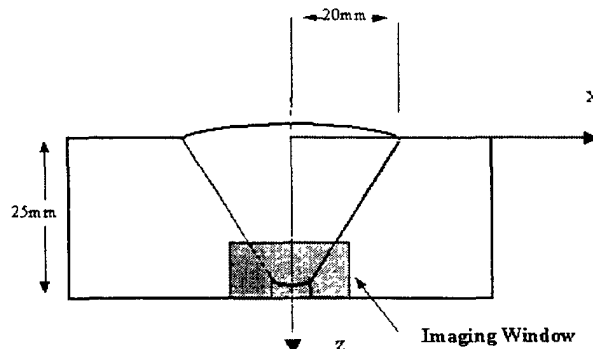
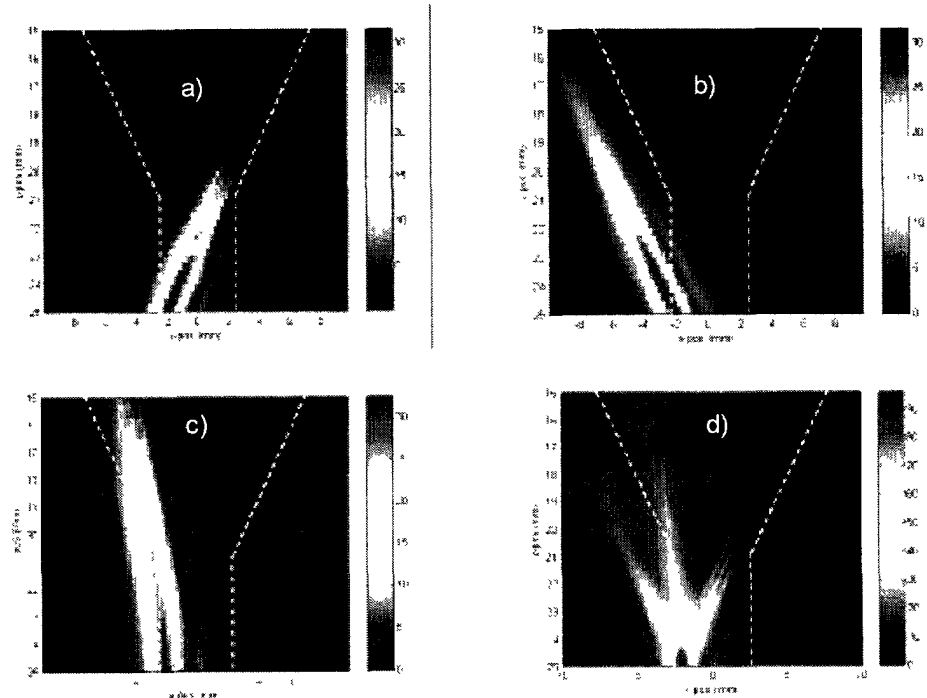
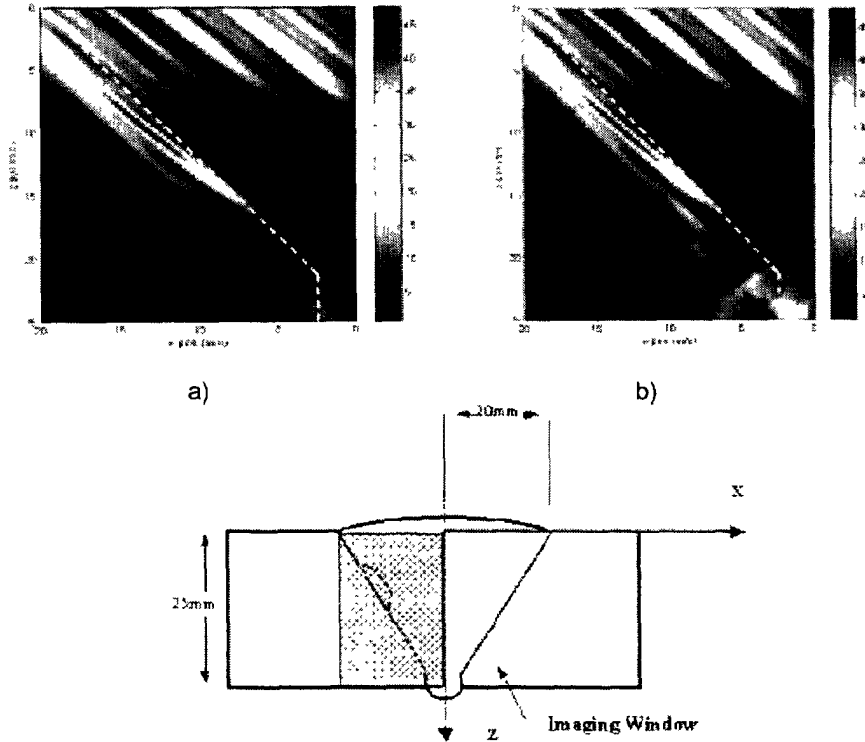


Figure 8. Multi-path SAFT results for flaw #2

Lack of penetration results were computed with paths (0,0), (1,1), (0,1) (1,0). Focusing effect of the multi-path image reconstruction is shown in Figure 8d where all paths were considered. Accuracy in the flaw sizing was highly improved when using all wave paths to reconstruct the flaw at a threshold of  $-6\text{dB}$ . Setting the threshold was arbitrary, however, an important parameter to accurately calculate the size of the flaw.

Figure 9 shows images of lack of fusion weld flaws computed with single and multi-paths at  $10^\circ$  beam spread angle. In Figure 8a, wave path (0,0) was employed for the image reconstruction. However, paths (0,0), (0,1) and (1,1) were considered for the computation of Figure 8b. It was clearly noted that, the contributions of all paths were weak compared to path (1,1). This was caused by the highly oriented nature of the lack of fusion flaw.



**Figure 9.** Multi-path SAFT results for defect #3

Table 5 summarizes all flaw dimensions computed with multi-path SAFT. From the multi-path SAFT image computation for flaws #2 and #3, a very small error in the flaw length and depth at  $-6\text{dB}$  and  $-2\text{dB}$  image thresholds were obtained. However, in the case of flaw #4 (slag inclusion flaw), flaw dimensions were difficult to obtain. The multi-reflections that occur on the complex shape of the flaw boundaries make it difficult to interpret the computed image. Using SAFT with this type of flaws requires careful and more appropriate signal acquisition.

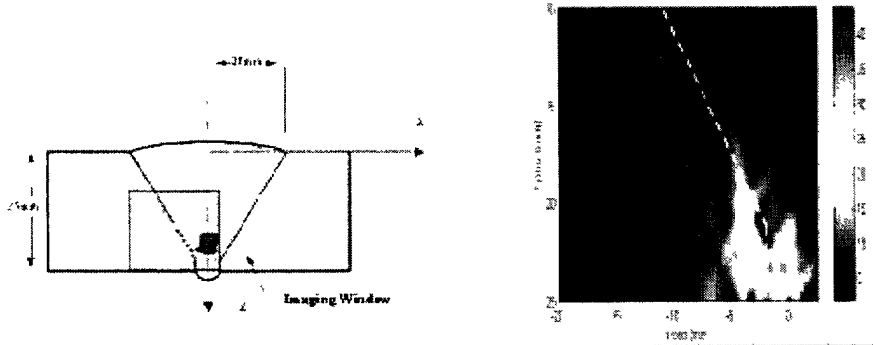


Figure 10. Multi-path SAFT results for defect #4

Table 5. Flaw characterization with SAFT using PE setup

Flaw	Depth			Height		
	Measured	Real	Error	Measured	Real	Error
1	N/a	Surface	N/a	N/a	0.4"	N/a
2	0.903"	0.935"	0.03"	0.09"	0.1"	0.01"
3	0.29"	0.3"	0.005"	0.19"	0.2"	0.004"
4	N/a	0.75"	N/a	N/a	0.1"	N/a

## CONCLUSIONS

The principle of multi-path SAFT was investigated using pulse-echo setup to detect common pipeline weld defects. SAFT results were compared to TOFD and time-of-flight tests.

Compared to the TOFD and PE results, the multi-path SAFT algorithm presented good accuracy for two flaws. The use of the reconstruction helped to increase focusing and the effective testing aperture. In the case of highly oriented or complex surface flaw, the SAFT theoretical accuracy could not be reached, since, only some few scattered rays are received. Improvement of the inspection mode while using SAFT should help to improve the accuracy. Currently, a split angle pitch-catch version of the algorithm is being tested.

Critical algorithm parameters have also been identified (reconstructed image threshold, beam width limitation, wave velocity and wedge delay). Our experimental results showed that, a practical use of the multi-path SAFT requires a specific and careful testing procedure to calibrate these critical parameters.

## REFERENCES

- 
- <sup>1</sup> PANDA system see <http://www.tektrend.com/products/products/panda.html>
  - <sup>2</sup> R.N Thomson, Transverse and longitudinal resolution of the synthetic aperture focusing technique, ULTRASONICS, Jan. 1984
  - <sup>3</sup> F. Ganansia, A.Chahbaz and K. Mborokih, "Experimental Evaluation of Weld Defects Using Multi-Path SAFT," QNDE, Montreal. 25 July 1999
  - <sup>4</sup> J.P. Charlesworth, J.A.G. Temple," Engineering Application of Ultrasonic TOFD" RSP, John Wiley